August 27, 1992

PROPOSAL FOR THE DETECTION OF RELATIVISTIC ANTI-HYDROGEN ATOMS PRODUCED BY PAIR PRODUCTION WITH POSITRON CAPTURE

THE ANTIHYDROGEN COLLABORATION

C. T. Munger

Stanford Linear Accelerator Center

M. Mandelkern, J. Schultz

University of California at Irvine

T.A. Armstrong, M. A. Hasan, R. A. Lewis and G. A. Smith

Pennsylvania State

ABSTRACT

We propose to detect the first antihydrogen atoms. The integrated luminosity expected in 1994 of 200 pb^{-1} for $\bar{p}p$ annihilation in the E760 hydrogen gas target will produce a sample of 10^3 antihydrogen atoms. These atoms exit the accumulator in a low emittance, neutral beam which will be detected by an apparatus set up in the gap between the accumulator and debuncher rings. We believe the antihydrogen can be detected with essentially unit efficiency and zero background; the total cost of the project is roughly \$300K. The proponents expect to share costs. We request only a few shifts of protons to make a hydrogen beam with which to calibrate our apparatus, but the experiment is otherwise wholly parasitic on E760 and needs no new beam time.

INTRODUCTION

Antihydrogen, the simplest atomic bound state of antimatter, $\bar{H} \equiv (e^+\bar{p})$, has never been observed. A long sought goal of atomic physics is to produce sufficient numbers of antihydrogen atoms to confirm the CPT invariance of bound states in quantum electrodynamics; in particular, one wants to verify the equivalence of the $2S_{1/2} - 2P_{1/2}$ Lamb shift splittings of H and $\bar{H}$.

Sources for the production of $\bar{H}$ have been proposed based on the radiative capture of slow positrons with antiprotons [1] , a process which can be enhanced by laser stimulation [27] , or based on charge exchange in the collision of an antiproton with positronium [3] ; or based on three-body recombination in dense $\bar{p}$-e^+ plasmas;

however, none of these methods has yet been shown thus far to work in practice. We note that relativistic $\bar{H}$ atoms may be produced in the collision of antiprotons with ordinary atoms. An antiproton passing through the Coulomb field of a nucleus of charge Z will create electron-positron pairs; occasionally the positron will appear in a bound instead of a continuum state about the antiproton and form antihydrogen. The cross section for this process, $\sigma(\bar{p}Z \rightarrow \bar{H}e^{-}Z)$, is calculated in Appendix 1 and is roughly $\sim 5\ Z^2$ pbarn for antiproton momenta above ~ 2 GeV/c.

Ironically, it appears that a practical source of antihydrogen based on pair production with positron capture already exists. The experiment E760 will integrate in 1994 a luminosity for $\bar{p}p$ annihilation of $200\,\mathrm{pb}^{-1}$ at the Fermilab accumulator using an internal H_2 gas target; a serendipitous byproduct will be a sample of 1000 antihydrogen atoms. This antihydrogen appears in a low emittance, neutral beam and can be detected with essentially unit efficiency and zero background by an apparatus located in the gap between the accumulator and debuncher rings and wholly separate from E760.

As methods of cooling antiproton beams improve, so will the achievable antihydrogen flux. We note a sample of a few 10^4 antihydrogen atoms would suffice to measure the antihydrogen Lamb shift to a precision of $\sim 1\%$, and thus probe for anomalous, CPT-violating $e^{+}\bar{p}$ interactions that could cause level shifts equal to $1 \cdot 10^{-8}$ of the antihydrogen binding energy. The first detection of antihydrogen is a necessary step toward that goal. Because protons can also be circulated in the FermiLab accumulator, one can form a relativistic hydrogen beam and Lamb shifts of hydrogen and antihydrogen in the same atomic beam apparatus. The method of measuring the Lamb shift is outlined in Appendix 3.

Properties of the Fermilab $\bar{H}$ beam.

The momentum transferred to the antiproton in the process $\bar{p} + Z \rightarrow \bar{H} + e^{-} + Z$ is small, the order of $mc \sim 5 \cdot 10^{-4}\,\mathrm{GeV/c}$. The momentum and position vectors of an antihydrogen atom are therefore the same as those of the antiproton from which it forms; the antihydrogen therefore emerges in a beam with the same tiny momentum spread, $\delta p/p \sim 2 \cdot 10^{-4}$, as the circulating antiproton beam. Experiment E760, when operated at an antiproton momentum of $\gtrsim 3\,\mathrm{GeV/c}$ achieves a beam height in the gas target (at A50) with $\sigma_y = 0.25\,\mathrm{cm}$, and an angular distribution with $\sigma_\theta = 1.9 \cdot 10^{-4}$ radian [18] . After 14.5 meters flight, sufficient for the neutral antihydrogen beam to exit the first bend magnet [29] (at A5B3) and pass undeflected out of the accumulator ring, the beam height is $\sigma_y \approx 0.28\,\mathrm{cm}$. That is fortunately small enough for the beam to stay within the beam pipe (vertical half-width 2.3 cm) until it reaches the dipole. Even 40 meters from the gas target the spot size is only $\sigma_y \approx 1.1\,\mathrm{cm}$, and it is smaller yet for higher antiproton momenta. One extracts a charge-separated, monoenergetic, small-emittance antihydrogen beam. Outside the accumulator ring the equipment used to detect antihydrogen will not interfere with E760, and target-related backgrounds will be attenuated by distance.

Heating of the circulating antiproton beam by multiple Coulomb scattering establishes one bound to the maximum density of hydrogen gas allowed to E760. The cross section for the antiproton to Coulomb scatter, and the cross section for it to

form antihydrogen, both scale roughly as Z^2. If the allowable target density is limited by heating therefore one cannot increase the flux of antihydrogen by choosing a (necessarily) rare high-Z instead of a dense low-Z target gas [10] . However the ratio of the number of inelastic nuclear events to the number of antihydrogen atoms formed does diminish as $A^{2/3}Z^{-2}$, where A is the target atomic number. Because the number of scattered target electrons and attendant bremsstrahlung photons also diminishes, roughly as $1/Z$, atomic sources of target-related backgrounds are also suppressed. The antihydrogen yield per circulating antiproton also increases from $\sim 2 \cdot 10^{-10}$ to $\sim 2 \cdot 10^{-8}$. If E760 chooses to run a different target gas our experiment will only run better.

Antihydrogen easily survives transit through laboratory magnetic fields. It forms mostly in atomic s states populated with a probability expected to diminish with principal quantum number n roughly as $1/n^3$. The magnetic field of a bend magnet generates a large electric field in the antihydrogen rest frame and an s state may ionize. In a uniform electric field the rate of ionization of a state with parabolic quantum numbers [8] n, n_2, m is [14]

$$R \sim \frac{1}{n^3 n_2!\,(n_2+|m|)!}\left(\frac{n^3F}{4}\right)^{-2n_2-|m|-1} e^{3(n-2n_2-m)-2/(3n^3F)}\,\frac{\alpha^2 mc^2}{\hbar}$$

where F is the applied electric field in units of $e^2/a_0 = 5.142 \cdot 10^9$ Volt/cm and a_0 is the Bohr radius. Ionization proceeds by the tunneling of a positron out of a Coulomb potential well and so there is a drastic dependence of the ionization rate on the well depth and so on the principal quantum number n. Even for the maximum accumulator momentum of 8.83 Gev/c and dipole strength of 16.7 kguass the rest ionization rate of the $1s$ state is $4.3 \cdot 10^{-13}$ sec^{-1}, and so it easily survives extraction. The most stable of the $n = 2$ states by contrast ionizes with a rest rate of $6.4 \cdot 10^{+14}$ sec^{-1}, and so travels only some 5 microns. The Lorentz transform of even earth's meager magnetic field of ~ 1 gauss, let of alone fringe fields from accelerator magnets, will mix the metastable $2s$ state with the nearly degenerate $2p$ and induce an electric dipole transition to the $1s$ state with a rate of $\sim 6.3 \cdot 10^8$ sec^{-1}. Most initial $2s$ population will therefore transfer to the $1s$ before the first bend magnet, and so contribute to the extracted antihydrogen.

Antihydrogen easily survives passage through the gas target and subsequent laboratory vacuum. Fast antihydrogen disassociates when it collides with an atom into a free positron and antiproton. Data for the disassociation cross section for monatomic hydrogen beams [11] , extrapolated to a beam momentum of 3 GeV/ c, yield disassociation cross sections of $2.5 \cdot 10^{-20}$ cm^2, $2.7 \cdot 10^{-19}$ cm^2, and $3.3 \cdot 10^{-19}$ cm^2 per H_2, N_2, and CH_4 target molecule, respectively. The probability that an antihydrogen atom will disassociate before exiting the E760 H_2 gas target, of column density 10^{14} atoms/ cm^2, is less than 10^{-4} even if the target consists entirely of microdroplets of $\sim 10^5 - 10^6$ molecules per droplet [12] and if all the antihydrogen atoms are created inside a droplet. Plainly as one learns to cool beams at a greater rate one is free to increase in proportion the target density (or the target nuclear charge) and so

the rate of antihydrogen formation, certainly up to antihydrogen fluxes of $> 1\,\mathrm{sec}^{-1}$. Transport of antihydrogen requires only rough vacuum: 10 meters travel through 1 millitorr of nitrogen equivalent will disassociate only $\sim 1\%$ of the antihydrogen beam.

Detection of Antihydrogen

Fast antihydrogen separates in solids into a free particle pair much more readily than any other particle can. It separates with a probability > 0.99 in a mere membrane of polyethylene 400 microgram/cm^2 thick [13] . The probabilities a photon converts or a hadron interacts in such a thin membrane are only $\sim 2.7 \cdot 10^{-5}$ and $6.6 \cdot 10^{-7}$ [14] , respectively. The momentum transfer which separates antihydrogen is small, and so an antihydrogen atom generates in coincidence, from some point in a known, few-square-centimeter area of a membrane possibly tens of meters from the gas target, a positron and an antiproton with a common and tightly constrained velocity equal to the velocity of the circulating antiprotons in the ring. So spectacular is this signature that the chief difficulty in designing an apparatus to detect antihydrogen is to choose which of many sufficient schemes is the simplest. For the sake of discussion we assume the antiproton beam has a momentum of 3 Gev/c; the apparatus we propose can accomodate any momentum in the accumulator range of 3 to 9 Gev/c merely by scaling remotely the various magnetic fields.

After being freed, the light positron scatters significantly in the membrane while the heavy antiproton does not, the latter retaining the small momentum spread of the accumulator, $\delta p/p \sim 2 \cdot 10^{-4}$. Despite the initial Fermi momentum of the $1s$ state, the momentum transfer in the collision which frees the positron, and subsequent large-angle and (multiple) small-angle scattering of the positron in the membrane, more than 99% of the positrons exit in a ± 0.10 radian cone about the antiproton direction [15] . The nominal kinetic energy of the positrons, 1.200 MeV, is smeared by the longitudinal Fermi momentum of the $1s$ state, $\langle p_t^2 \rangle^{1/2} = \sqrt{1/3}\alpha mc$, by $\sigma_K = 6.9\,\mathrm{keV}$, which incidentally is larger than even the average 1.4 keV the positron loses traversing the membrane [16] . It is easy to stop the positrons in a scintillator < 2 mm thick and generate, with $\sim 90\%$ efficiency, a signal with a time resolution of $\sigma_t < 1$ ns and energy resolution $\sim 20\%$. The signal from the other 10% of the positrons may be lost because the a positron can backscatter out of the scintillator [17] .

A layout of our apparatus to detect antihydrogen may be found in Figure 2. The components easily fit in the gap between the accumulator and debuncher rings as indicated in Figure 1. After its extraction from the accumulator ring an antiproton flies a further 3 meters through a "filter" magnet, whose function described later, and into a vacuum chamber. The antihydrogen hits a 400 microgram/cm^2 membrane and disassociates into a positron and an antiproton. The membrane sits in a weak magnetic field which bends and focusses the monoenergetic positrons with ~ 1 meter flight path into a scintillator a few centimeters in diameter. This first scintillator is backed by a sodium iodide detector to veto the passage of any more penetrating particles and to catch one of the 511 keV photons from the positron's subsequent 2γ annihilation [19] . The antiproton continues through a pair of multiwire proportional chambers (MWPC's), each with 1 mm position resolution, separated by a 5° bend magnet. We seek a momentum resolution of 2%. The antiproton also passes through

a pair of scintillators which measure its transit time and so its velocity. A pair of scintillators 30 meters apart with individual timing resolutions of $\sigma_t = 150$ ps provides 21 standard deviations of $\bar{p}\pi^-$ separation at a common momentum of 3 GeV/ c and 7 standard deviations at 6 Gev/c. The timing resolution for these scintillators can be small because the antiproton spot diameter is small and its position measured by the MWPC's. The antiproton also passes through a ring-imaging high-pressure Čerenkov detector of DISC [30]type. This detector will provide a signal only for particles within ± 1 milliradian of the nominal antiproton direction and within $\delta\beta/\beta \approx 1 \cdot 10^{-4}$ of its nominal velocity. (The momentum resolution of the stochastically cooled antiproton beam, $\delta p/p = 2{\cdot}10^{-4}$, corresponds to a velocity resolution $\delta\beta/\beta = 2{\cdot}10^{-5}$ at 3 Gev/c.) The DISC detector can handle an antiproton of any velocity merely by scaling the gas pressure. An antihydrogen event is defined by hits in the MWPC's consistent with a antiproton of the right momentum coming from the ring, by scintillator and Čerenkov hits consistent with a particle of the right velocity vector, and by a hit in the positron scintillator with the correct time and the correct energy deposit together with the absence of a hit in the veto for more penetrating particles.

Several general circumstances make such a simple scheme plausible, despite the $\sim 4 \cdot 10^9$ times larger cross section for $\bar{p}p$ annihilation, instead of for antihydrogen formation, in the E760 gas target. Positive particles with momenta equal to the antiproton are deflected by the $A5B3$ magnet away from the antihydrogen beam. No neutral particle except antihydrogen can both survive 10 meters of flight and decay within the apparatus into an antiproton, so the mere presence of an antiproton, tagged by its momentum and velocity, establishes (if the ambient flux of antiprotons lost from the ring is low enough) the passage of a neutral antihydrogen atom. The antiproton momentum, velocity, and time of arrival are set to known and adjustable values by the tune of the $\bar{p}$ ring, as are the positron energy and time of arrival. Combinations of hits from decays of particles in flight, and hits from particles created from beam lost from the accumulator, mimic continuous distributions of these quantities. Kinematics dictate that neutrals produced in $\bar{p}p$ or $\bar{p}n$ collisions will rarely decay into charged particles with momenta as high as the original antiproton momentum. Still more rarely will a decay produce at once a hard GeV/c and a soft Mev/c particle, because of the large difference in energy scales. The application of these general considerations to the elimination of some obvious particle backgrounds may be found in Appendix 3. Importantly, a second 400 microgram/ cm^2 membrane set upstream of the first will remove all antihydrogen from the beam but leave all backgrounds unchanged [32] . The extra "filter" magnet between the accumulator ring and our vacuum box deflects the antiproton freed when this second membrane is lowered, so the antiproton is not accepted by our apparatus. This test will eliminate a false signal of antihydrogen from any apparatus.

Modifications to the accumulator

These are minor. The neutral antihydrogen beam presently runs into the vacuum pipe within the first 5° bend magnet, A5B3, after the $E670$ gas target. The separation at the end of the magnet between antiproton beam, centered in the beampipe, and the antihydrogen beam is 2.62," while the half-width of the existing pipe is only 1.90". We believe that the existing beampipe can be replaced by a "Y", as shown in Figure 3a, to let the neutral beam escape without the need to make a new magnet. As is

shown in Figure 3b the new pipe does not intercept the coils of the magnet, though it does squeeze the space now filled by heating coils and thermal insulation which together allow bakeout of the beampipe.

The pair of RF cavities between A5B3 and A5Q4 also intercept the antihydrogen beam and will have to be moved. There is fortunately available a site, fully equivalent given the six-fold symmetry of the acumulator lattice, upstream of E760, between A4B3 and A4Q4. This site is shown in Figure 1. Both the present and proposed sites lie under the A5 service building and so it may not be necessary to move the utilities supplying the cavities.

From our arm of the "Y" we will hang an isolation valve and a few meters of beampipe terminating in a box which contains the membrane which will disassociate the antihydrogen and the detector for the freed positrons. When the E760 gas target is not running we will valve off our arm of the "Y" a meter or so from the dipole magnet. While the gas jet of E760 is running, the vacuum box, membrane, and positron detector must be exposed to the vacuum of the accumulator because of the large stripping cross section for antihydrogen and because of the short range of the freed few-Mev positrons. The accumulator vacuum is then, however, already compromised by the gas jet. Because the antihydrogen spot size is the order of 1 centimeter we can use a small-diameter, low-conductance pipe from the "Y" to our vacuum box, which pipe will isolate to some degree our vacuum from that of the accumulator.

The layout of our beamline between the accumulator and debuncher rings is shown in Figure 2. Once past the dipole magnet and the RF cavities there is roughly 30 meters free flight for antihydrogen in the gap between the rings. At a convenient point past the A5B3 magnet we will diassociate the antihydrogen in a membrane and bend the freed antiproton through roughly 5° so it parallels the beamline of the accumulator. Most of the space between the accumulator and debuncher rings will then be left clear to preserve easy access to the beamlines.

To calibrate our apparatus with a hydrogen, instead of antihydrogen, beam we request that the accumulator be run for some shifts with protons circulating in the direction in which antiprotons usually circulate, and with the E760 gas target on. Radiative electron capture in the E760 target then makes 1700 hydrogen atoms a day, assuming an equal proton as antiproton average currents, with which to calibrate our apparatus. Our apparatus can accomodate hydrogen as well as antihydrogen by inverting the polarity of our magnetic fields.

Demands made upon E760

It does not matter at what beam momenta from 3 to 9 Gev/c E760 chooses to run, or how often the beam momentum is changed. Our production cross section is flat over this momentum range, and our apparatus will accomodate any momentum merely by scaling remotely the strength of the bend magnets and adjusting the gas pressure in the the Čerenkov detector. It does not matter what target gas E760 uses. Motion of the beam position in the gas target by a few millimeters poses no problem. We do ask that the inclination of the antiproton beam through the gas target be monitored and stable to less than 1 milliradian so that the antiproton spot doesn't swing by more than 1 centimeter after 10 meters flight, so we can build an

apparatus with a narrow angular accepatance for antiprotons and so that we can build a Čerenkov detector with a tight velocity window, $\delta\beta/\beta < 10^{-4}$.

As mentioned earlier, we will need E760 to run its gas target for some shifts while protons are circulated in the accumulator.

Status of other experiments seeking antihydrogen at LEAR

One hundred physicists gathered in Munich July 30, 1992 for a two-day workshop to study methods of making antihydrogen. No other apparatus which might make antihydrogen is even being designed at present. Not only are sources of sufficient cold positrons and antiprotons not available, but the mechanisms proposed to make antihydrogen (radiative combination $\bar{p} + e^+ \rightarrow \bar{H} + \gamma$; combination in a plasma, $\bar{p} + 2e^+ \rightarrow \bar{H} + e^+$; and formation using positronium, $\bar{p} + (e^+e^-) \rightarrow \bar{H} + e^-$) have not been made to yield simple hydrogen, despite the obvious availability of electrons and protons. Synthesis of antihydrogen by means other than that we propose therefore requires the successful union of at least three independent and still nascent technologies. No one at the conference thought success possible within three years; five seems more likely. We think Fermilab has a commanding lead. With the Lamb shift experiment outlined in Appendix 2, Fermilab may find in the future a similar lead in the first spectroscopy of antihydrogen

Costs

We seek to establish a plausible upper bound to the costs; obviously we will scrounge everything we can. A breakdown may be found in Table II. We judge the total cost to be $300K.

Resources: Manpower and money

The proponents of this experiment are willing to share costs. SLAC in particular will contribute 1 year's salary for Charles Munger and 15K seed money; he has no other commitments. The experiment is both interesting and small, so we believe sufficient funding will be available if Fermilab deems the experiment compatible with its research program. At a miniumum we expect Fermilab to pick up the cost of the essential modifications to the accumulator: the "Y" on the vacuum system, the relocation of the RF cavities, and the modifications to the bakeout jacket for the dipole magnet.

Appendix 1 : Cross Section Calculation [36]

It is straightforward to relate the cross sections, viewed in the antiproton rest frame, for pair creation with capture into the 1s state, $\bar{p} + Z \rightarrow \bar{H}(1s) + e^- + Z$, and for the corresponding photon reaction, $\gamma + \bar{p} \rightarrow e^- + \bar{H}(1s)$, using the equivalent photon approximation [5] . In this approximation

$$\sigma_{Z+\bar{p}\rightarrow Z+e^-+\bar{H}(1s)} = \frac{2Z^2\alpha}{\pi\omega} \int_{2m}^{\omega_{max}} \ln\left(\frac{\gamma M}{\omega}\right) \sigma_{\gamma+\bar{p}\rightarrow e^-+\bar{H}(1s)}(\omega) \frac{d\omega}{\omega}, \qquad (1)$$

where Z is the nuclear charge, γ is the usual relativistic factor (energy/mass) for the moving nucleus, ω is the photon energy in the antihydrogen rest frame, and m and M are the masses of the electron and antiproton, respectively.

The invariant helicity amplitude for the photon-induced capture reaction $\gamma + \bar{p} \to e^- + \bar{H}(1s)$ is precisely related by crossing symmetry to the corresponding helicity amplitude for the photoionization of hydrogen, $\gamma + H(1s) \to e^- + p$; one need only interchange the Mandelstam variables s and u; i.e.,

$$|M|^2_{capture}(s,t,u) = (1/2)|M|^2_{photo}(u,t,s), \tag{2}$$

after summing and averaging the spins.

We define the kinematics for the capture reaction $\gamma + \bar{p} \to e^- + \bar{H}(1s)$ in the $\bar{p}$ rest frame as follows: ϵ is the energy of the outgoing electron, $\vec{p}$ and $\vec{k}$ are the momentum vectors respectively of the outgoing electron and incoming photon (with $p \equiv |\vec{p}|$ and $\omega \equiv |\vec{k}| = k$), and θ is the angle between the momentum vectors. The Mandelstam variables for the capture reaction are expressed in terms of the $\bar{p}$ rest frame variables through the relations

$$\begin{aligned} s &= M^2 + 2M\omega, \\ t &= m^2 - 2\omega\epsilon + 2\omega p\cos\theta, \\ u &= M^2 - 2\epsilon M + m^2, \end{aligned} \tag{3}$$

where ω is the photon energy, and where ϵ, p, and θ are respectively the electron's recoil energy, three-momentum, and production angle.

The matrix elements for photoionization are well known [4]. After expressing all the relevant quantities in terms of the Mandelstam variables, performing the crossing $s \leftrightarrow u$, and substituting the $\bar{p}$ rest frame variables, we obtain

$$\begin{aligned} |M|^2_{capture} = \frac{(32\pi)^2\alpha^6 m^4 M^2}{2(\vec{p}-\vec{k})^4} \Bigg\{ & \frac{2\pi m}{\epsilon + m}\left[a^2p^2 + a\frac{(\epsilon+m)}{m}(\vec{k}\cdot\vec{p} - p^2)\left(\frac{1}{k^2-p^2} + \frac{1}{(\vec{k}-\vec{p})^2}\right)\right. \\ & \left. + \frac{(\epsilon+m)^2}{4m^2}(\vec{k}-\vec{p})^2\left(\frac{1}{(\vec{k}-\vec{p})^2} + \frac{1}{k^2-p^2}\right)^2\right] \\ & -\pi\frac{\epsilon+m}{m}\frac{p^2\sin^2\theta}{(k^2-p^2)(\vec{k}-\vec{p})^2} + 2a\pi\frac{p^2\sin^2\theta}{(\vec{k}-\vec{p})^2}\Bigg\}. \end{aligned} \tag{4}$$

The quantity a is given by

$$a = \frac{1}{(\vec{k}-\vec{p})^2} + \frac{\epsilon}{m(k^2-p^2)}. \tag{5}$$

If the cross section for capture is calculated in the antiproton rest frame, and the photoionization cross section is calculated in the hydrogen atom rest frame, then

within the approximations we are making (small electron mass m and energy ϵ with respect to the proton mass M) the flux factors for these two processes are equal. Thus the total cross section for the photon-induced capture reaction is

$$\sigma_{\gamma+\bar{p}\to e^-+\bar{H}(1s)}(\omega) = \frac{1}{64\pi^2 M^2\omega}\int \epsilon p|M|^2_{capture} d\cos\theta. \tag{6}$$

After numerical integration of equation (1) using (6) we obtain the results shown in Table 1 for the cross section for capture into the $1s$ state. The cross section for $\bar{p}Z \to \bar{H}(1s)e^-Z$ is approximately $5Z^2$ pbarn for antiproton momenta above ~ 2 GeV/c. Capture into states of higher principal quantum number we expect will increase the total cross section for capture by $\sim 10\% - 20\%$.

For large γ we can compare our results with those obtained by Bertulani and Baur [6]. For $\gamma = 200$ they calculate a cross section of 6.7 pb, which is not far from our result of 7.3 pb. For lower values of γ there is a greater discrepancy, because they obtain $\sigma(\gamma = 100) = 5.3$ pb and $\sigma(\gamma = 50) = 3.8$ pb.

The above results can also be applied to calculate the cross section for electron capture in heavy ion collisions, $Z_1 + Z_2 \to (Z_1 e^-) + Z_2 + e^+$, where the electron has been captured in the $1s$ state of the nucleus Z_1. In addition to the factor of Z_2^2 from the equivalent photon approximation, we need to scale our results by the wavefunction factor [6]

$$F = Z_1^5 \frac{(2\pi\alpha Z_1)}{e^{2\pi\alpha Z_1} - 1}, \tag{7}$$

which is $\approx Z_1^5$ for $\alpha Z_1 \ll 1$.

Appendix 2: Target-related backgrounds

One hundred $\bar{p}p$ annihilations at 3 GeV/c produce some 400 charged particles, 100-200 π^0's, 6 strange particles and 7 $\bar{n}n$ pairs [20] . Backgrounds are primarily suppressed by the small solid angle subtended by the membrane and by the acceptance aperture for an antiproton after stripping; an active area 1 cm in radius 20 meters from the target subtends a fraction of 4π solid angle of only $6 \cdot 10^{-8}$. Of neutral particles which might pass through the magnets and collimators, only neutrons, photons, K_L's, and antineutrons survive to enter them–Λ's and K_S's have $1/e$ attenuation lengths of at most 19.2 cm and 18.4 cm and are attenuated by more than $2 \cdot 10^{-23}$ over a distance of 10 meters. The neutrons cannot mimic the $\bar{p}e^+$ signal for antihydrogen; the effects of the other neutrals we consider in more detail.

Neutrals rarely convert to charged particles within the geometric acceptance of the apparatus. Photons, converting in the membrane to e^+e^-, and K_L decays, like $K_L \to \pi^- e^+ \nu_e \to \mu^- \bar{\nu}_\mu e^+ \nu_e$, might mimic antihydrogen, if the positron made were soft and if a hard negative particle were misidentified as an antiproton. Of photons passing through the membrane only $\sim 2 \cdot 10^{-5}$ can convert because it is so thin. Of K_L's aimed to pass though the membrane, because of the K_L $1/e$ decay length of

~ 10.6 meter, one finds that at most $\sim 1.3 \cdot 10^{-4}$ can decay within the $\pm \sim 5$ cm of the membrane, supposed to be necessary if the positron is to curl into its scintillator. Antineutrons, copiously produced ($\sigma \approx 2.0$ mbarn) in the forward direction by the two-body charge exchange reaction $\bar{p}p \rightarrow \bar{n}n$, can produce both a 3 GeV/c antiproton and an ~ 1 MeV positron via the beta-decay $\bar{n} \rightarrow \bar{p}e^{+}\nu$ [25] . However due to the long antineutron half-life the probability one decays within ± 5 cm of the membrane is only $\sim 4 \cdot 10^{-11}$. Because a momentum of roughly 200-300 MeV/c is typically transferred in charge exchange the forward antineutrons are distributed over an angle of roughly 10^{-2} radian and so the probability that an antineutron which decays at the right distance also passes within the $\sim 10^{-4}$ radian acceptance of the apparatus is smaller by another factor $\sim 10^{-4}$.

Even if a neutral converts within the geometric acceptance of the apparatus it will seldom convert to particles with the right momenta to mimic the disassociation of antihydrogen. The spectrum of photons with energies above $2m$ is dominated by photons from π^0 decay and not from the bremsstrahlung of target electrons, generated either as the electrons are accelerated in the field of the moving antiproton or as the electrons subsequently stop in the beam pipe. From the cross section for π^0 production we calculate that there are the order of $3 \cdot 10^{-3}$ conversions per square centimeter of membrane per antihydrogen produced. To produce an electron with a momentum equal to the antiproton momentum requires a photon with laboratory energy greater than 3 GeV. Kinematics dictate that photons can rarely be boosted to that energy. For example, even a favorable two body reaction $\bar{p}p \rightarrow 2\pi^0$ with one pion aimed down the beampipe will produce a ≥ 3 GeV photon but a third of the time. Furthermore photon conversion has a roughly flat spectrum as a function of final electron momentum, so a ~ 3 GeV photon will produce an electron with a momentum within 1% of 3 GeV only $\sim 1\%$ of the time. It will produce a soft positron within the model 1.20 ± 0.24 MeV energy acceptance of the positron scintillator only $\sim 0.02\%$ of the time. The background from photon conversions is plainly negligible.

Consider next the background from K_L decay. At most of order 10^{-2} K_L's per antihydrogen atom decay within ± 5 cm of the membrane per square centimeter of membrane. Kinematics again dictate that a π^- from $K_L \rightarrow \pi^- e^+ \nu$ will rarely be boosted to a momentum of 3 GeV/c; such a boost is for example forbidden if the $\bar{p}p$ annihilation produces four pions as well as two kaons. Even if the pion is so boosted the recoil positron and neutrino momenta in the decay $K_L \rightarrow \pi^- e^+ \nu$ will rarely conspire to give a laboratory positron energy as soft as 1.2 MeV.

The kinematics of the decay of antineutrons generated from charge-exchange are not so favorable. Because the $\bar{n} - \bar{p}$ mass difference is so small, both the antineutron and the decay antiproton automatically carry the full original $\bar{p}$ momentum. The laboratory kinetic energy of the decay positron ranges only from 0 to 7.6 MeV, so our model ± 0.24 MeV scintillator measurement of the positron kinetic energy is only somewhat effective in suppressing the background. Fortunately as has been shown the number of antineutrons decaying within the apparatus is so small that the background may be neglected.

Exotic bound systems, such as hypothetical bound states of mesons, cannot mimic the signal for antihydrogen. These will not have velocities equal to the velocity of the antiprotons in the ring. They are also too tightly bound to diassociate in the the

membrane; even the electromagnetically bound, instead of strongly bound, system $(\pi^+\mu^-)$, observed in the decay of neutral kaons, has a probability of disassociating of only 0.1.

We conclude that there are no obvious backgrounds which preclude the detection of antihydrogen, and, inasmuch as the individual counters in our model experiment are all of high efficiency, the antihydrogen may be detected with near-unit probability. The effect of random backgrounds from antiprotons lost from the accumulator must be explored, but it will be difficult for them to satisfy our multiple coincidences; the random overlap rate between two counters with rates of 1 kHz (we note the accumulator beam is essentially continuous) and time windows of 10 ns is about 3 per year, and we have no fewer than four counters: the positron scintillator, the two TOF scintillators for the antiproton, and the DISC detector. There is ample freedom to elaborate the apparatus (more tracking and more scintillators for the antiproton, an antiproton calorimeter, addition of magnetic focussing for the positron or a positron magnetic spectrometer, 4π detection of positron annihilation radiation, etc.) should the random rates recorded in the accumulator tunnel by test apparatus be high.

Appendix 3: Future antihydrogen experiments and the Lamb Shift

The process of pair creation with capture has itself never been seen and its measurement is of interest. The first observation of the analogous process in the collision of ordinary nuclei, $Z_1 + Z_2 \rightarrow (Z_1 e^-) + e^+ + Z_2$, is the subject of an experiment soon to run at the Lawrence Berkeley Laboratory BEVALAC [26] , and the process is predicted to be a major source of beam loss at the Relativistic Heavy Ion Collider [28] . However the primary motivation for experiments studying antihydrogen [21]remains to test the CPT theorem. We note that by changing the polarity of the magnets in the Fermilab accumulator one can circulate protons in the same sense as antiprotons, and compare hydrogen to antihydrogen in the same apparatus. The dominant process [33] for charge exchange at momenta of 3 GeV/c is radiative electron capture, where an essentially free electron in the target gas falls into the $1s$ state of the moving proton and the excess energy is given up by radiating a photon. The cross section [34] per target electron is $\gtrsim 1.7$ nanobarn, so for equal circulating currents through an H_2 gas target the hydrogen beam will have ~ 340 times the intensity of the antihydrogen beam.

We outline two experiments which seem practical with samples of order 10^3 and 10^4 antihydrogen atoms. The first is a measurement of the rate of field ionization of the $n = 2$ states in an electric field provided by the Lorentz transform of a laboratory magnetic field. Perhaps 10% of a 3 GeV/ c antihydrogen beam in the $1s$ state can be collisionally excited into states with $n = 2$ by passing it through a thin membrane. If the membrane sits in a 20 kgauss transverse magnetic field, states with $n > 2$ will ionize instantly, the states with $n = 2$ will ionize with $1/e$ decay lengths of order 10 cm, and the $1s$ state will not ionize at all. The distance a states with $n = 2$ flies before ionizing is marked by the a deflection of the freed antiproton by the magnetic field by an amount between the zero deflection of the surviving $1s$ component of the beam and the large deflection of the antihydrogen which ionizes instantly or disassociates in the membrane. Ten centimeters of flight before disassociation changes the deflection of the antiproton seen 3 meters away by 6.7 cm–many times the antiproton spot size

of $\lesssim 1$ cm. The distance a state flies is also marked by the freed positron, whose orbit radius is only 2mm in the transverse field and which can be directed into some sort of position-sensitive detector. The positron and antiproton have of course their usual unique energy. A flux of a few thousand $\bar{H}$'s may be sufficient to measure the three distinct field ionization rates of the $n = 2$ states to $\sim 10\%$. Because the ionization rate is a tunneling process it is surprisingly sensitive to details of the antihydrogen wavefunction; a 10% shift would require for example a change in $\langle r \rangle$ for the $n = 2$ states of only 0.24%.

We note that ionization in a magnetic field can be efficiently used to count $n = 2$ states without counting states of different principal quantum number. (No laser for example has sufficient continuous power to photo-ionize efficiently the relativistic antihydrogen beam.) By driving the 1000 Mhz $2s - 2p$ transition and monitoring the surviving $2s$ population as a function of frequency one can measure the antihydrogen Lamb shift. For a beam with $\gamma = 3$ the $1/e$ decay length of the $2p$ states is 1.35 meters, so a few meters from an excitation membrane only the metastable $2s$ population survives. One can conveniently drive the Doppler-shifted transition by chasing the beam with 6.1 GHz radiation aimed down a roughly 10 meter long, 4-by-2 cm cross section waveguide; this guide also serves as a beam pipe. Modest laboratory powers [31] of roughly 10 Watt/cm^2 will mix the $2s$ state completely with the $2p$ and to make the $2s$ decay with a $1/e$ distance of $\gtrsim 2.7$ m. To prevent Stark mixing of the $2s$ and $2p$ states, transverse magnetic fields must be less than 0.1 gauss from the excitation membrane down the length of the guide until the sharp rise of the transverse magnetic field used to ionize the $n = 2$ state. Little of the $2s$ state will decay radiatively in the rise if the rise occurs over less than the fully mixed $2s$ decay length of 2.7 meters. A sample of a few hundred antihydrogen atoms in the $2s$ state would suffice to determine the antihydrogen Lamb shift to $\sim 1\%$. Such a sample would be provided by a flux of roughly 10^4 antihydrogen atoms if the excitation target yields as expected [35]0.01 $2s$ states per incident $1s$. The experiment would be sensitive to a differential shift of the $2s$ and $2p$ states of hydrogen and antihydrogen equal to a fraction $\sim 2 \cdot 10^{-8}$ of the states' binding energy.

REFERENCES

[1] See for example : H. Poth, "Synthesis of Antihydrogen".

[2] H. Poth, Appl. Phys. A43, 287 (1987), and references therein.

[3] B. I. Deutch et al., Hyperfine Interactions 44, 271 (1988); M. Charlton, Phys. Lett. A143, 143 (1990).

[4] V. B. Berestetskii, E. M. Lifshitz and L.P. Pitaevskii, "Relativistic Quantum Theory, Part 1", (second edition, Pergamon Press), page 212. A missing factor of 2 has here been restored to their formulae; see for example *The Quantum Theory of Radiation, Third Edition*, W. Heitler, Oxford, 1954, p. 209.

[5] Ref. 4, page 438.

[6] G. Bertulani and C. A. Baur, Z. Phys. A330, 77 (1988); Phys. Rep. 163, 299 (1988). See also: J. Eichler, Phys. Rep. 193, 255 (1990).

[7] See e.g. S. J. Brodsky, J. F. Gunion, and D. E. Soper, Phys. Rev. D36, 2710 (1987); S. J. Brodsky and A. H. Mueller, Phys. Lett. B206, 685,(1988); R. Vogt, S. J. Brodsky, and P. Hoyer, Nucl. Phys. B360 67 (1991), and SLAC-PUB-5827 (1992).

[8] H. Bethe and Salpeter, *Quantum Mechanics of One- and Two-electron Atoms*, N. Y. Academic Press, 1957.

[9] "Theory of the ionization of the hydrogen atom by an external electric field," T. Yamabe, A. Tachibana, and H. J. Silverstone, Phys. Rev. A **16**, 877(1977). The formula is these author's equation 125, and represents the asymptotic behavior of the ionization rate in the limit of small field F. See also "The model dependence of the ionization rate of hydrogen in a uniform electric field," R. Haydock and D. R. Kingham, J. Phys. B **14**, 385(1981). Phys. Rev. A **16**, 877(1977).

[10] The rate of heating by Xenon is roughly a factor of 2 greater than naive Z^2 scaling of the heating by hydrogen would suggest. The hydrogen nucleus can recoil slightly where the heavy Xenon nucleus cannot, and the tight charge distribution of the 1s screens the nuclear charge more effectively than the more diffuse distribution of a many-electron atom.

[11] See *Collisional Electron Detachment from Hydrogen Atoms between 22 and 45 Mev*, by E. Acerbi, C. Birattari, B. Candoni, M. Castiglioni, D. Cutrupi and C. Succi, Lettre al Nuovo Cimento **10**, 598 (1974). See also *Systematics of atom-atom collisions strengths at high speeds*, by George H. Gillespie and Mitio Inokuti, Phys. Rev. A. **22**, 2430 (1980). In the Born approximation where $Z\alpha/\beta << 1$ even for relativistic beams all cross sections scale as $1/\beta^2$, where β is the hydrogen beam velocity, except for possible factors involving $\ln(\gamma)$ whose variation may be neglected.

[12] M. Macri, *A Clustered H_2 beam*, in *Proceedings of CERN Accelerator School*, Geneva, 1983.

[13] In fact the membrane required to achieve this degree of detachment is probably a factor ~ 3 thinner. In a solid target where the time between collisions is much shorter than the radiative lifetime of excited states, any excitation to a bound state leads immediately to a subsequent stripping. The measure $\langle r^2 \rangle$ for the atomic size of the $2p$ state, for example, is 10 times that of the $1s$, and $\langle r^2 \rangle$ varies asymptotically as n^4 for large principal quantum number n. The cross section for excitation is twice the cross section for direct ionization of the $1s$ state in a collision with a bare nucleus of charge Z [24] ; one may expect a similar ratio for collisions with a screened nucleus. The conditions of Acerbi *et. al.* [11] were such that only the cross section for direct excitation was measured.

[14] Values of 14.70 $\mathrm{gm\,cm^{-2}}$ and $60.2\,\mathrm{gm\,cm^{-2}}$ for the radiation length and nuclear collision length in carbon are taken from Review of Particle Properties, *Physics Letters B* **239**, 1990, Table III.5

[15] A scatter through > 0.10 radian requires a transfer of transverse momentum much greater than the (transverse) Fermi momentum of the $1s$ state and so the probability for such a scatter may be calculated using the formula for simple Rutherford scattering; the probability is $\sim 8 \cdot 10^{-3}$ for a 400 microgram/ cm^2 carbon target. This angle is safely more than three standard deviations of the gaussian distribution from small-angle multiple scattering. The contribution to the angle of the (transverse) momentum distribution of the $1s$ state, $\langle p_t^2 \rangle^{1/2} = \sqrt{2/3}\alpha mc$, is negligible.

[16] The dE/dx of a 1.20 MeV electron in carbon, which we use to estimate that of a positron, is $3.67\,\mathrm{MeV\,cm^2\,gm^{-1}}$. See L. Pages, E. Bertel, H. Joffre, L. Sklavenitis, *Atomic Data* **4**, 1(1972).

[17] An energy deposit of $0.1 - 0.2$ MeV has been found to be adequate to establish a signal using positrons, so some of the backscattered positrons may still generate a timing signal. The backscatter probability from silicon instead of carbon is ~ 0.25 instead of 0.10. (Ali Belkacem and Harvey Gould, private communications) For a survey experiment with a low count rate it seems therefore unwise to try to measure the positron energy with a surface barrier detector instead of its arrival time with a scintillator.

[18] Values adapted from *Prospects for $\bar{p}p$ Experiments in the TEV I Accumulator*, John Peoples, Jr., in *Low Energy Antimatter, Proceedings of the Workshop on the Design of an Low Energy Antimatter Facility*, David B. Cline, editor, World Scientific, 1986.

[19] Merely backing a scintillator with a sodium iodide crystal generates a 511 keV signal (including both the full-energy peak and the Compton tail) some 75% of the time. Ali Belkacem, private communication.

[20] *Numerical Data and Functional Relationships in Science and Technology, Volume 12a,b: Total Cross Sections for the Reaction of High-Energy Particles*, Springer-Verlag, 1988.

[21] See *Possible Experiments with Antihydrogen*, Reinhard Neumann, in *Fundamental Symmetries*, P. Bloch, P. Pavlopoulos, and R. Klapisch, eds., Plenum Press, New York (1987)

[22] For a brief overview of the design see [21]. The primary reference seems to be H. Poth, *Supplements to Proposal P86 (Berger et. al.,1985)*, CERN/PSCC/86-21, CERN/PSCC/86-37.

[23] Preprint, *Precision Measurements of Charmonium States formed in $\bar{p}p$ Annihilation*, FERMILAB-Pub-91/299-E, E760, November, 1991 (Submitted to Physical Review letters), Table I, and private communications.

[24] The calculation of the cross section for the disassociation or excitation of monatomic hydrogen in a collision with bare nucleus of charge Z is a classic problem first analysed by Bethe (H. Bethe, *Z. Phys.***76**, 293 (1932)) For an exposition in english see N. F. Mott and H. S. Massey, *The Theory of Atomic Collisions*, Oxford, Clarendon Press, 1987. For an overview of the theory including atomic screening, with application to the stripping of $(\pi\mu)$ atoms see M. K. Prasad, *Acta Physica Polonica* **B10**, 635(1979).

[25] The authors are indebted to Michael Peskin for noting the potential significance of this background.

[26] Ali Belkacem and Harvey Gould, private communication. The experiment is described in Lawrence Berkeley Laboratory BEVALAC proposal 954H.

[27] See *Observation of Laser-Induced Recombination in Merged Electron and Proton Beams*, U. Schramm, J. Berger, M. Grieser, D. Habs, E. Jaeschke, G. Kilgus, D. Schwalm, A. Wolf, R. Neumann and R. Schuch, Phys. Rev. Lett. **67**, 221991, and *Experimental Observation of Laser-Stimulated Radiative Recombination*, F. B. Yousif, P. Van der Donk, Z. Kucherovsky, J. Reis, E. Brannen, J. B. A. Mitchell, and T. J. Morgan, Phys. Rev. Lett. **67**, 26 (1991).

[28] RHIC Conceptual Design Report BNL 52195, table IV.3-10 and pp.118-120. Also see BNL 52247 UC-414 (High Energy Physics-DOE/OSTI-4500-R75), the proceedings of the workshop *"Can RHIC be used to test QED?"*, M. Fatyga, R.J. Rhoades-Brown, and M. J. Tannenbaum, editors, April 20-21, 1990.

[29] *Design Report, Tevatron 1 Project, September 1984*

[30] See for example *Čerenkov Counter Technique in High-Energy Physics*, J. Litt and R. Meunier, in Annual Review of Nuclear Science **23**, 1973.

[31] The formula for the required power is equation (26) in W. E. Lamb, Jr., and R. C. Retherford, Phys. Rev. **60**, 817 (1941).

[32] Even the exotic bound state of a pion and a muon, formed in the decay $K^0 \rightarrow (\mu^+\pi^-)\nu_\mu$ and its charge conjugate, strips only $\sim$ 10% of the time in such a membrane.

[33] See *Mechanisms for charge transfer (or for the capture of any light particle) at asymptotically high impact velocities* , R. Shakeshaft and L. Spruch, Rev. Mod. Phys. **51**, 369, (1979).

[34] The cross section for radiative capture of a free electron with Lorentz factor γ onto a charge Z is

$$\sigma_r c = 4\pi\alpha^4 Z^5 \left(\frac{e^2}{mc^2}\right)^2 (\gamma-1)^{-5/2}(\gamma+1)^{+1/2} \times \left[\frac{4}{3} + \frac{\gamma(\gamma-2)}{\gamma+1}\left(1 - \frac{1}{2\gamma(\gamma^2-1)} \ln \frac{\gamma+(\gamma^2+1)}{\gamma-(\gamma^2-1)}\right)\right]$$

This formula is adapted from a formula found in G. Raisbeck and F. Yiou, Phys. Rev. A **4**, 1958, 1971, after correcting for several errors these authors made transcribing the relativistic matrix element. See for example Heitler, *The Quantum Theory of Radiation*, Oxford, 1954, equation V.22.45, and the original reference, F. Sauter, Ann. d. Phys. **9**, 454, (1931), equation 39.

[35] A precise calculation has not been made. Calculations for the cross sections for Coulomb excitation and stripping of several Gev/c hydrogen indicate the maximum hydrogen $2s$ yield is close to 1%. The yield of $2s$ hydrogen and antihydrogen in the same target may differ, because the hydrogen can exchange electrons in the target while the antihydrogen cannot exchange positrons.

[36] Ivan Schmidt, Stanley Brodsky, and Charles Munger

γ	σ (pbarn)
200	7.3
100	6.9
50	6.4
10	5.3
5	4.8
2	4.2

Table I

Cross section (σ) for the production of anti-hydrogen in the 1s state by antiprotons incident on a proton target, as a function of the Lorentz factor γ of the antiproton.

For other targets the cross section scales as Z^2.

Item	Cost ($K)
Vacuum pipe "Y" and membrane box	30
UHV all-metal pneumatic isolation value	4
UHV line for the antiproton, 20 meters	10
Cryo pump for the box and antiproton line	8
Cryo pump valve, viton seal	5
Changing the bakeout coils and insulation of the D3 magnet	7
Relocation of the RF cavities	???
Filter magnet (to be scrounged)	0
Two UHV compatible membrane mounts with remote actuators	5
Magnetic field coils for guiding the positrons	5
Positron scintillator	4
Pair of NaI detectors for detecting annihilation radiation	16
TOF scintillators and phototubes for the antiproton line	4
Laser and fiber optics to calibrate timing	15
Pair of MWPC's with 1 mm x and y resolution	8
Antiproton bend magnet (to be scrounged)	0
Gas Cerenkov detector of DISC type	60
Stand-alone system for data acquistition	35
Contingency	?50?
	—
Total	256K ±?

Table II

Breakdown of Costs for the Antihydrogen exeriment, in thousands of dollars. Items tagged with question marks are uncertain or unknown.

Figure Captions

Figure 1

Approximate layout of the Antihydrogen Beamline. Shown is the flight of the neutral antihydrogen beam (dotted line) and the flight of the component antiproton after stripping. Because we are free to choose the site and strength of the magnet which bends the component antiproton the layout may be altered freely; the roughly 4-by-30 meter corridor between the Debuncher and Accumulator rings offers enough room to set up the equipment. The site to which we propose moving the RF cavities is shown.

Figure 2

An expanded view of Figure 1, showing the layout of the apparatus along the antihydrogen beamline. The individual components are not to scale.

Figure 3

Shown is the proposed "Y" in the beampipe superimposed on a top view of an assembly drawing of the A5B3 dipole magnet. Shown on a different scale is a cross section at the end of the magnet through the magnet and new beam pipe. The size and separation of the antiproton and antihydrogen spots are shown. (See drawing number 8020-ME-196482 and the Design Report, Tevatron 1 Project, Figure 12-1).

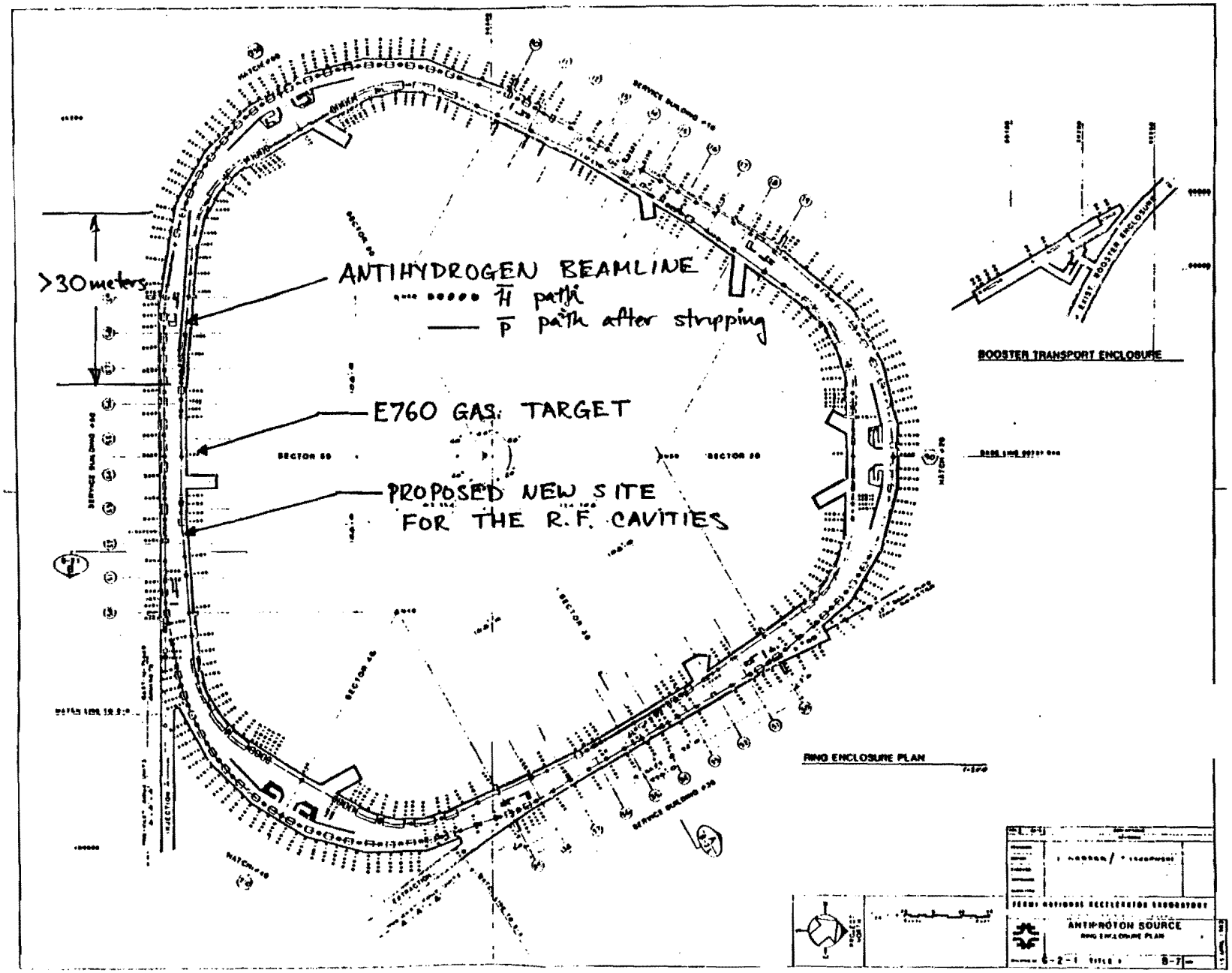
>30 meters
ANTIHYDROGEN BEAMLINE
$\bar{H}$ path
$\bar{p}$ path after stripping
E760 GAS TARGET
PROPOSED NEW SITE
FOR THE R.F. CAVITIES
BOOSTER TRANSPORT ENCLOSURE
RING ENCLOSURE PLAN
ANTIPROTON SOURCE

FIGURE 1

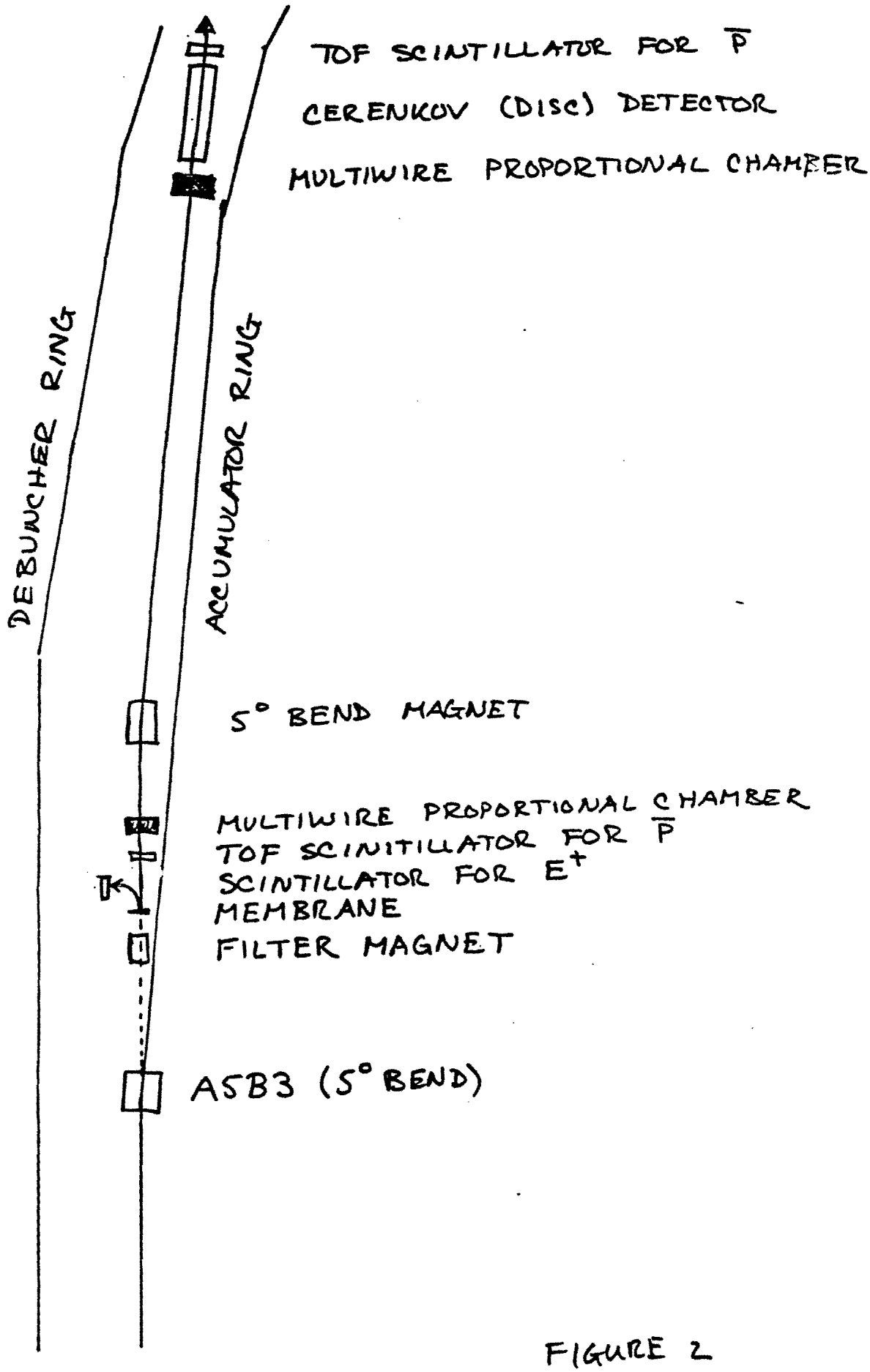
TOF SCINTILLATOR FOR $\bar{P}$
CERENKOV (DISC) DETECTOR
MULTIWIRE PROPORTIONAL CHAMBER
DEBUNCHER RING
ACCUMULATOR RING
5° BEND MAGNET
MULTIWIRE PROPORTIONAL CHAMBER
TOF SCINITILLATOR FOR $\bar{P}$
SCINTILLATOR FOR E^+
MEMBRANE
FILTER MAGNET
A5B3 (5° BEND)

FIGURE 2

(a)

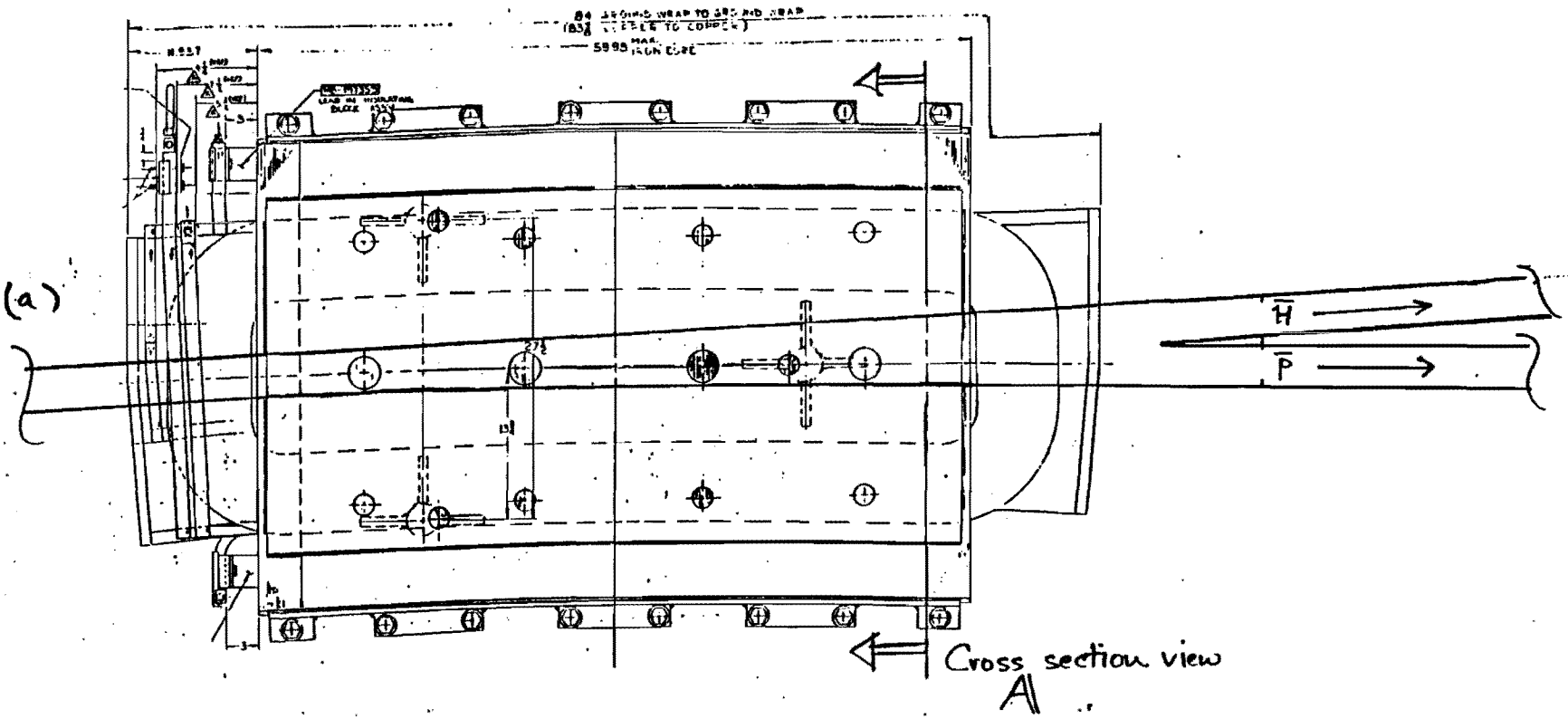

(b)

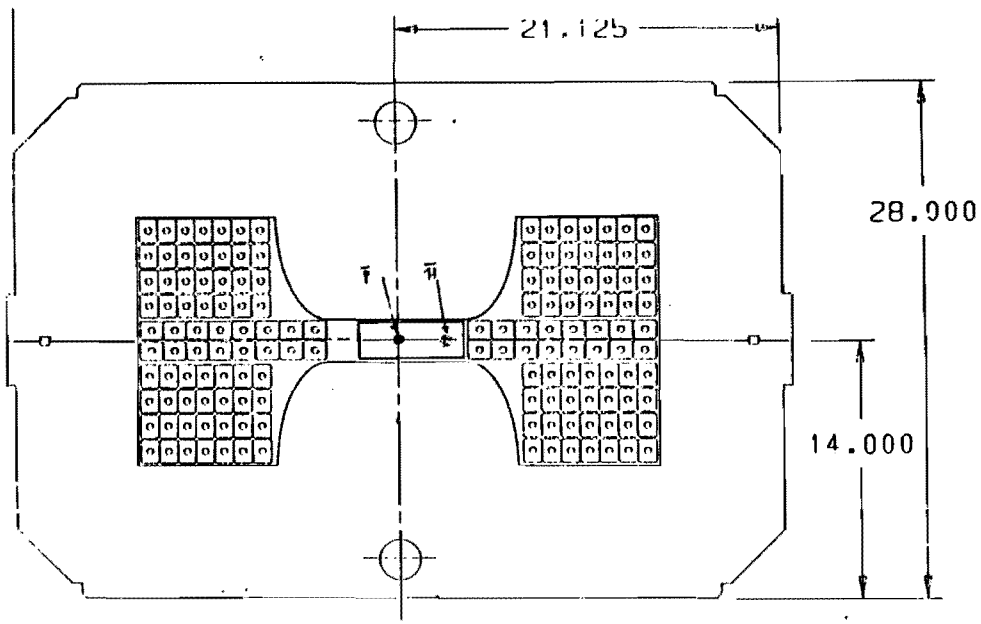

FIGURE 3 a, b